

NICMOS Narrow-band Images of OMC-1

A.S.B. Schultz¹, Sean W.J. Colgan, E.F. Erickson, M.J. Kaufman, D.J. Hollenbach

NASA-Ames Research Center, Moffett Field, CA 94035

C.R. O'Dell

Department of Space Physics and Astronomy, MS-108, Rice University, 6100 S. Main St.,

Houston, TX 77005-1892

E.T. Young, H. Chen

Steward Observatory, University of Arizona, Tucson, AZ 85721

Received _____; accepted _____

¹and SETI Institute

ABSTRACT

We present images of a $90'' \times 90''$ field centered on BN in OMC-1, taken with the Near-Infrared Camera and MultiObject Spectrograph (NICMOS) aboard the *Hubble Space Telescope*. The observed lines are H_2 1-0 S(1), $P\alpha$, [FeII] $1.64 \mu\text{m}$, and the adjacent continua.

The region is rich in interesting structures. The most remarkable are the streamers or “fingers” of H_2 emission which extend from $15''$ to $50''$ from IRc2, seen here in unprecedented detail. Unlike the northern H_2 fingers, the inner fingers do not exhibit significant [FeII] emission at their tips, which we suggest is due to lower excitation.

These observations also show that the general morphology of the $P\alpha$ and [FeII] emission (both imaged for the first time in this region) bears a striking resemblance to that of the $H\alpha$ and [SII] emission previously observed with WFPC2. This implies that these IR and optical lines are produced by radiative excitation on the surface of the molecular cloud. The $P\alpha$ morphology of HH 202 is also very similar to its $H\alpha$ and [OIII] emission, again suggesting that the $P\alpha$ in this object is photo-excited by the Trapezium, as has been suggested for the optical emission.

We find evidence of shock-excited [FeII] in HH 208, where it again closely follows the morphology of [SII]. There is also H_2 coincident with the [SII] and [FeII] emission, which may be associated with HH 208.

Finally, we note some interesting continuum features: diffuse “tails” trailing from IRc3 and IRc4, more extensive observations of the “crescent” found by Stolovy, et al. (1998), and new observations of a similar oval object nearby. We also find a “V”-shaped region which may be the boundary of a cavity being cleared by IRc2.

1. Introduction

As the nearest region ($d=450\text{pc}$) undergoing recent massive star formation, the Orion giant molecular cloud is the target of intense study at many wavelengths. On the edge of the OMC-1 molecular cloud is a blister HII region: a bubble of ionized gas, excited by the Trapezium stars. The visible nebula is the thin layer of photo-ionized gas on the surface of the molecular cloud. Between the HII region and the molecular cloud lies a photodissociation region (PDR) which is also excited by the Trapezium. A lid of neutral gas covers the entire nebula (Van der Werf & Gross 1989).

Within the molecular cloud behind the HII region lies BN/KL, a location of particular interest both because of the candidate protostars identified there and because of the associated energetic outflows. The energetics of the region seem to be dominated by a few luminous but deeply embedded sources whose bolometric luminosities approach $10^5 L_{\odot}$ (e.g. Genzel & Stutzki 1989). The outflows appear to originate from the vicinity of the radio continuum sources "I" and "n", located $\approx 8''$ SE of BN (Menten & Reid 1995). With the exception of the bright near-IR sources IRc2, BN, and IRc9, the extended continuum features in the region appear to be due to reflected starlight (Minchin et al. 1991) seen through inhomogeneities in the surrounding dust cloud.

Here we introduce and briefly discuss new [FeII] ($1.64 \mu\text{m}$), $P\alpha$ ($1.87 \mu\text{m}$), H_2 1-0 S(1) ($2.12 \mu\text{m}$) and continuum images of a region centered on BN/KL. These images were obtained with the Near-Infrared Camera and MultiObject Spectrometer (NICMOS) on board the *Hubble Space Telescope*. The images have a pixel size of $0.2''$ and show fine details in all of the filters.

H_2 emission arises either from shocked gas (where it traces both dissociative ($v_S \gtrsim 50 \text{ km s}^{-1}$) and non-dissociative ($v_S \lesssim 50 \text{ km s}^{-1}$) shocks, or from UV fluorescence. [FeII] emission arises from dissociative shocks as well as photoionized gas. $P\alpha$ emission is

typically from recombinations in HII regions, but can also result from high-velocity shocks.

2. Observations and Data Reduction

The data were obtained with NICMOS Camera 3 in two separate orbits of the *Hubble Space Telescope* on 12 and 16 Jan 1998. The total area of each frame is $50'' \times 50''$, with a plate scale of $0.2''$ per pixel. The diffraction limit ($\theta = 1.22\lambda/D$) is $0.2''$ at $2 \mu\text{m}$. Images were obtained in three line filters, plus three nearby continuum filters (all filters are 1% bandpass): [FeII] $1.64 \mu\text{m}$ (F164N), $1.66 \mu\text{m}$ (F166N), $P\alpha$ $1.87 \mu\text{m}$ (F187N), $1.90 \mu\text{m}$ (F190N), H_2 1-0 S(1) $2.12 \mu\text{m}$ (F212N), and $2.15 \mu\text{m}$ (F215N).

The data were taken in the NICMOS MULTIACCUM mode; total integration time per frame was 32s for F212N and F215N, 16s for F187N and F190N, and 88s for F164N and F166N. The data were processed with the standard NICMOS CALNICA pipeline, which includes bias-subtraction, dark-subtraction, flat-fielding, cosmic-ray removal, and flux calibration. The continuum images were then subtracted from the emission-line images.

The H_2 and $P\alpha$ images are each composed of seven frames, covering a total of approximately $95'' \times 95''$. The [FeII] images are composed of four frames, covering the central square arcminute of the H_2 and $P\alpha$ images. In all cases the position angle was 356 degrees east from north. After mosaicing, the various filters were registered to the orientation and position of the F215N filter using star positions (with an accuracy of ≈ 0.2 pixel). The resulting 3σ upper limits in Jy in a 1 square arcsecond area are: $1.0\text{E-}5$ for F215N, $1.3\text{E-}5$ for F212N, $2.5\text{E-}5$ for F190N, $3.4\text{E-}5$ for F187N, $0.5\text{E-}5$ for F166N, and $0.6\text{E-}5$ for F164N.

3. Results

Overviews of the region are shown in Figures 1-3. Figure 1 is a schematic highlighting the important features in the region. Figure 2 shows our large field, which includes H₂, P α , and 2.15 μ m continuum. The smaller field, comprised of H₂, P α , and [FeII] images, is shown in Figure 3.

The interesting structures in our images can be divided roughly into three groups: shocked emission features (the H₂ fingers, HH 208), radiative emission features (the “wisp”, HH 202, proplyds, and the proplyd cloud), and continuum features (IRc3 and IRc4, the crescent, and the “V”).

3.1. Shock Excitation Features

3.1.1. H₂ Fingers

The most striking feature of the data is the remarkable array of H₂ “fingers” emanating from the general vicinity of BN (Fig. 2). Allen & Burton (1993) (AB hereafter) first discovered structures like these up to 2 arcmin (0.25 pc) north of our field. They interpreted the fingers as bow shocks formed in a stellar outflow, when a “bullet” of ejected matter strikes the ambient medium. Based on the H₂ cooling time, AB concluded that the fingers were created in a single event, rather than by a precessing jet or succession of jets.

McCaughrean & Mac Low (1997) also present images of the region. They argue that the fingers are formed when a spherical wind is suddenly accelerated (e.g. by a second, faster wind behind it) into the ambient medium (Stone, Xu, & Mundy 1995). Rayleigh-Taylor instabilities form, fragmenting the cloud, and producing the fingers and bow shocks. Their model also predicts that the shell behind the fingers should break up into clumps.

To the north and northwest of BN we see a large area of flocculent emission, extending to roughly $45''$ from BN, with no definite finger structures. The H_2 emission is brightest in this region, which contains IRc9 and OMC Pk 1 (Beckwith, et al. 1978). This may be the clumpy emission behind the fingers predicted by Stone, Xu, & Mundy's model.

Our images (see Figure 2) reveal many of the fingers to be more complex than simple bow shocks. This is the "nested arc" structure seen in the inner fingers by Stolovy et al. (1998); we see these structures out to $50''$. The fingers exhibit delicate internal structures which may be only the superposition of separate fingers. The six H_2 fingers found by AB were all capped with [FeII] emission. This is understandable since the tip of the bow shock represents the region of greatest shock velocity, and therefore greatest excitation. Our [FeII] images cover only the central square arcminute of the area covered by our $2 \mu m$ observations, but within that region we find that only two of the fifteen H_2 fingers have [FeII] tips.

This is unlikely to be an extinction effect, even though the H_2 fingers are embedded in the molecular cloud; rather, the absence of [FeII] in the inner H_2 fingers is probably due to lower excitation. Unlike the northern fingers found by AB, the fingers in our image show the H_2 emission out to the tips of the bow shocks. This is consistent with other analyses of the shocked emission, which infer $\approx 40 \text{ km s}^{-1}$ non-dissociative shocks (Harwit et al. 1998). If the fingers were produced in a single outflow incident, as postulated by AB, the distant northern fingers may have traveled farther because of their larger velocity.

Shock models have been presented which predict the relative strengths of H_2 and [FeII] emission from dissociative shocks (e.g. Hollenbach & McKee 1989). For the two fingers in which we observe both [FeII] and H_2 emission, we find the observed ratios are consistent only with slow dissociative shocks ($v_S \lesssim 35 \text{ km s}^{-1}$).

3.1.2. HH 208

Most of the shocked [FeII] emission seen in our images is in HH 208. We find that the [FeII] emission is almost identical in morphology to the [SII] 6716/6730 Å emission seen by O'Dell et al. (1997a), which implies that the [FeII] and [SII] emission come from the same region: the photodissociation region (PDR) near the ionization front. The [FeII] emission cannot come from the HII region, because there Fe^+ would be converted to Fe^{++} ; the [SII] emission cannot come from very deep in the PDR because of extinction. Hence emission from both species probably originates in the PDR close to the far side (relative to the observer) of the ionization front. The presence of H_2 coincident with [FeII] and [SII] may also argue for the placement of HH 208 within the PDR, where radiative heating allows [FeII] and [SII] to be emitted from shocks at lower velocities than would be possible in colder gas; these shocks can excite H_2 without dissociating it.

We see at least one other example of an H_2 knot with a cap of [FeII] (which is also seen in [SII] by O'Dell et al. 1997a) to the SE of BN. We believe this to be a Herbig-Haro object; the [FeII] cap is the higher-excitation bow shock. For the same reasons applied to HH 208 above, this is also likely to be situated in the near side of the PDR.

3.2. Radiative Excitation Features

The general appearance of the $\text{P}\alpha$ and [FeII] emission is strikingly similar to that of $\text{H}\alpha$ and [SII] (O'Dell et al. 1997a). The maxima and minima of the $\text{H}\alpha$ emission are reproduced in $\text{P}\alpha$, with only a few important differences. The $\text{H}\alpha$ emission drops off sharply north of BN, whereas the $\text{P}\alpha$ decreases only toward the the northwest of BN. There is a particularly strong region of $\text{P}\alpha$ emission $\approx 40''$ SE of BN which is surrounded by 6 proplyds (see section 3.2.3). The differences between $\text{H}\alpha$ and $\text{P}\alpha$ are likely to be due to differential extinction.

3.2.1. The "Wisp"

One interesting structure found in $P\alpha$ and [FeII] emission is the bright "wisp" immediately to the northeast of BN (Figures 1 and 3). This object also appears in $H\alpha$, [SII], and [NII] 6583 Å (O'Dell et al 1997a). It was first observed with WFPC1 by Hester et al. (1991), who suggested it was a jet. The higher resolution WFPC2 images of O'Dell et al. (1997a), and the lack of high-velocity gas (O'Dell, Wen, & Hester 1991) show that this explanation is unlikely, but it is still unclear whether the gas is shock- or photo-excited.

Its appearance in hydrogen emission is different from that in the ionic lines; the hydrogen-emitting region is shorter and thicker than the ionic region. Furthermore, the [SII] and [FeII] images exhibit a second linear strand of emission, paralleling the main body and joining it in a faint emission knot at the western end. The [NII] image does not show this. Finally, the ionic emission region is offset slightly to the northeast from the hydrogen emission. This would be the case if the object is photo-excited from the south, since the more easily-excited species (hydrogen, in this case) would be seen closer to the Trapezium.

3.2.2. HH 202

Another feature seen in both optical and infrared wavelengths is HH 202, a large tubular structure in the southwestern corner of the field (Figures 1 and 2). This object was recently studied by O'Dell et al. (1997a), who note that while the lower-excitation lines of [SII] and [NII] are concentrated in the head of the long tube, [OIII] 5007 Å and $H\alpha$ emission is seen along the entire tube. O'Dell et al. (1997b) find that the [OIII] emission is blue-shifted. Our observations show that $P\alpha$, as well as very faint continuum emission at 1.90 μm and 2.15 μm , also extends the length of the tube.

O'Dell et al. (1997a, 1997b) suggest that the [OIII] emission along the tube does

not come entirely from shocks, but is partly photo-excited. They hypothesize a jet moving through the HII region, creating a tube that is photo-ionized from within by the Trapezium. Photo-ionization changes S^+ to S^{++} , so that the gas is unable to cool by [SII] emission (which its shock velocity would otherwise dictate), but must cool by emission of higher-excitation lines such as [OIII]. We suggest this radiative heating also produces the $P\alpha$ emission. The jet terminates in the neutral lid, producing the north and south knots which are bright in [SII] (O'Dell et al. 1997a, 1997b). We also find $P\alpha$ emission in the southern knot, with the same general position and morphology as the $H\alpha$ emission seen there by O'Dell et al (1997a). The higher-excitation lines of [OIII] and hydrogen are not seen in the northern knot.

3.2.3. Proplyds

The following proplyds all exhibit compact $P\alpha$ emission, suggesting that they are inside the ionized region: 113-153, 114-155, 115-155, 116-156, 131-247, 135-220, 138-207, 142-301, 154-240, 154-225, 163-249, 163-222, 165-235, 168-235, 170-249, and 173-236 (nomenclature of O'Dell & Wong, 1996). 142-301 is a striking object resembling an ice cream cone to the E of HH 202. We also find one compact object at the head of HH 202 which exhibits $P\alpha$ emission but does not have an optical counterpart (source P1 in Figure 1).

3.3. Continuum Features

3.3.1. IRc3 and IRc4

Both of these objects possess long, curving, diffuse "tails" of continuum emission extending to the southwest of the main objects (Figure 4). The brightest parts of the tails extend up to $13''$ (0.03pc) from the main objects, but there is much fainter emission up to

28" (0.06pc) away. The more distant features seem to emerge from behind curving strands of obscuration which lie to the southwest of BN (as well as to the south—these are best seen in Figure 2). Each of the bright tails is coincident with a finger of H₂ emission, which suggests the tails may be tunnels punched through the cloud by ejected matter that are now being illuminated from within by the exciting source.

3.3.2. *The Crescent*

In agreement with Stolovy et al. (1998), we detect the “crescent” feature in all three continuum images, with some associated H₂ emission. No [FeII] or P α emission is seen in this feature. The sensitive F166N image however (Figure 5), shows that the “tail” of the crescent extends up to 6" to the NW, 2.5" further than seen by Stolovy et al. Another, similar oval feature can be seen very faintly to the SE of the crescent. Its blunt end can be seen almost touching the NE extensions of BN.

The extended continuum source SEBN (Aitken et al. (1985), seen in Figure 4), approximately 25" East and 10" south of BN, exhibits a flocculent structure not as clearly delineated in previous images. This region has a large polarization ($\approx 30\%$ at K) whose orientation clearly points to illumination from the vicinity of IRc2 (Minchin et al. 1991). SEBN may be related to the general SE-NW outflows in the region.

3.3.3. *The V*

Approximately 7.5" northeast of BN and apparent in all three of the continuum images is the base (source q of Lonsdale et al. 1982) of a V-shaped structure which opens to the north (Figure 5). The extended ridge of dust emission mapped at 450 microns and 3.5 mm by Wright, et al. (1992) lies along the line joining BN and the apex of the V. The V is also

adjacent to the northeast extension of BN, which has a similarly sharp edge.

The V appears faintly in H₂ emission, but not in [FeII] or P α . The eastern branch contains a compact H₂ knot near its base and seems to terminate in a long H₂ feature. This linear structure appears to pass through a ring or bubble of H₂ emission and continue on the far side. Schild, Tennyson, & Miller (1997) suggested that this is a jet which struck a clump of denser material, producing an expanding density wave.

The coincident dust and H₂ emission suggest that the V is a photodissociation region. However, there is no known FUV emission from the center of the nebula, and no extended radio sources which would indicate a photo-ionized region obscured from our point of view, but with an unobscured path to the V. This renders a PDR interpretation unlikely. We propose a scenario in which the H₂ emission in the V is shock-excited. In this picture the supersonic outflow from the (unknown) central source clears a channel through the molecular cloud. Note that the angular extent of the general northern H₂ outflow region is bordered by the eastern leg of the V and by the H₂ jet. Thus the jet may delineate the confinement of the outflow by the molecular cloud. The continuum emission then results from the reflection of IR photons produced elsewhere in the cloud. The polarimetry of Minchin et al. (1991) seems to confirm the reflection hypothesis, and indicates that the V is likely to be illuminated by IRC2. In this picture the V shows the extent to which the outflow has been able to clear a path at its outer edges. The shocked H₂ emission it exhibits is from the impact of the outflow on the walls of the cavity.

4. Conclusions

We have seen that the near-IR emission in OMC-1 is complex, arising from structures at all levels of the nebula, from the HII region near the neutral lid, to deep within the underlying molecular cloud. The most striking features are the H₂ fingers, many of which

we see here in unprecedented detail. We find that most of the inner fingers do not exhibit detectable [FeII] emission, as the more distant northern fingers do (Allen & Burton 1993). We suggest that this is due to excitation, rather than extinction.

Our continuum images reveal numerous extended emission features which seem to be reflection from the continuum sources within the cloud, presumably including the outflow source. To the north of BN we see a V-shaped structure which lies at the eastern limit of the H₂ fingers, and may define the boundary of a cavity cleared by the outflow.

On the near side of the molecular cloud, within the PDR, we find shocked structures which exhibit both atomic ([FeII]) and molecular (H₂) emission, such as HH 208 and the [FeII]-capped H₂ knot to the SE of BN. The [FeII] morphology of these objects is very similar to their [SII] morphology seen by O'Dell et al. (1997a), implying that the objects are not buried deeply in the PDR.

The visible surface of the Orion Nebula, which is excited radiatively by the Trapezium stars, is seen in P α and [FeII], with a morphology strikingly similar to the H α , [SII], [OI], and [NII] emission found there by e.g. O'Dell, et al. (1997a). Embedded in this surface are a number of compact objects—proplyds—which exhibit P α emission.

Fig. 1.— Schematic of the OMC-1 region. Colors are as indicated.

Fig. 2.— Large field of OMC-1. Red is H_2 , green is $P\alpha$, and blue is $2.15 \mu\text{m}$ continuum.

Fig. 3.— Small field of OMC-1, showing H_2 (red), $P\alpha$ (green), and $[\text{FeII}]$ (blue) emission.

Fig. 4.— $2.15 \mu\text{m}$ continuum image of OMC-1.

Fig. 5.— $1.66 \mu\text{m}$ continuum in OMC-1, showing detail in the region around BN.

REFERENCES

- Aitken, D. K., Bailey, J. A., Roche, P. F., & Hough, J. H. 1985 MNRAS 215 815
- Allen, D.A. & Burton, M.G. 1993 Nature 363 54
- Beckwith, S., Persson, S.E., Neugebauer, G., & Becklin, E.E. 1978 ApJ 223 464
- Genzel, R. & Stutzki, J. 1989 ARA&A 27 41
- Harwit, M., Neufeld, D.A., Melnick, G.J., & Kaufman, M.J. 1998 ApJ 497 L105
- Hester, J.J., et al. 1991 ApJ 369 L75
- Hollenbach, D.J., & McKee, C. 1989 ApJ 342 306
- Lonsdale, C. J., Becklin, E. E., Lee, T. J., & Stewart, J. M. 1982 AJ 87 1819
- McCaughrean, M.J., & Mac Low, M.-M. 1997 AJ 113 391
- Menten, K.M., & Reid, M.J. 1995 ApJ 445 L157
- Minchin, N.R. et al. 1991 MNRAS 248 715
- O'Dell, C.R., Wen, Z., & Hester, J.J. 1991 PASP 103 82
- O'Dell, C.R. & Wong, S.K. 1996 AJ 111 846)
- O'Dell, C.R., Hartigan, P., Lane, W.M., Wong, S.K., Burton, M.G., Raymond, J., & Axon,
D.J. 1997a AJ 114 730
- O'Dell, C.R., Hartigan, P., Bally, J., & Morse, J.A. 1997b AJ 114 2106
- Schild, H., Miller, S., & Tennyson, J. 1997 A&A 318 608
- Stolovy, S.R., et al. 1998 ApJ 492 L151
- Stone, J.M., Xu, J. & Mundy, L.G. 1995 Nature 377 315
- Van der Werf, P.P. & Goss, W.M. 1989 A&A224 209

Wright, M., Sandell, G., Wilner, D.L., & Plambeck, R.L. 1992 ApJ 393 225

Schematic of the Near-IR Morphology of OMC-1

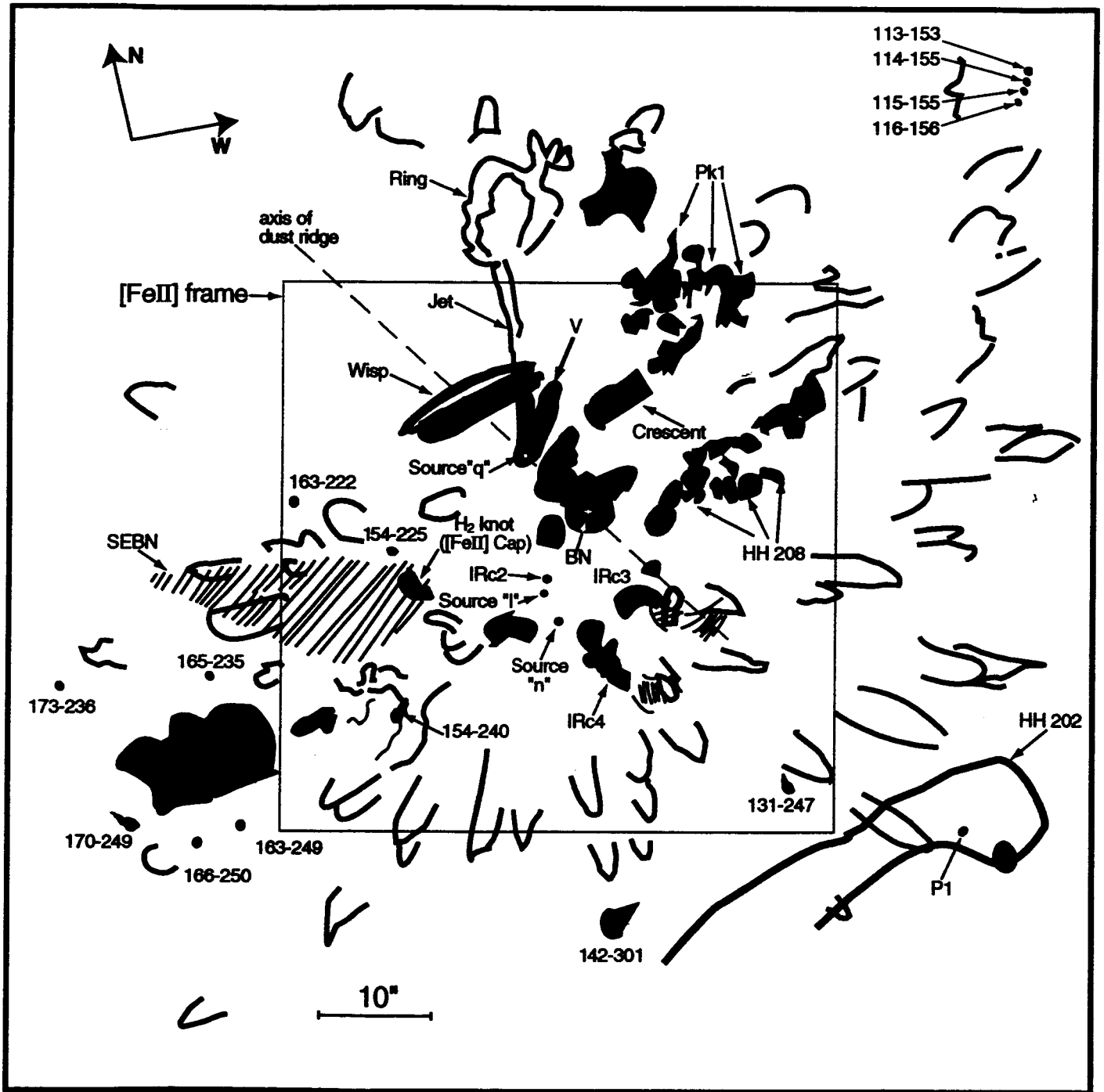
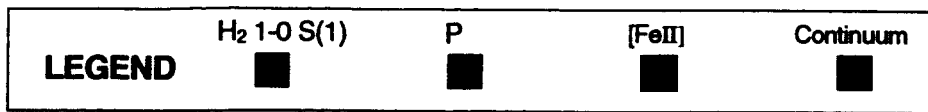
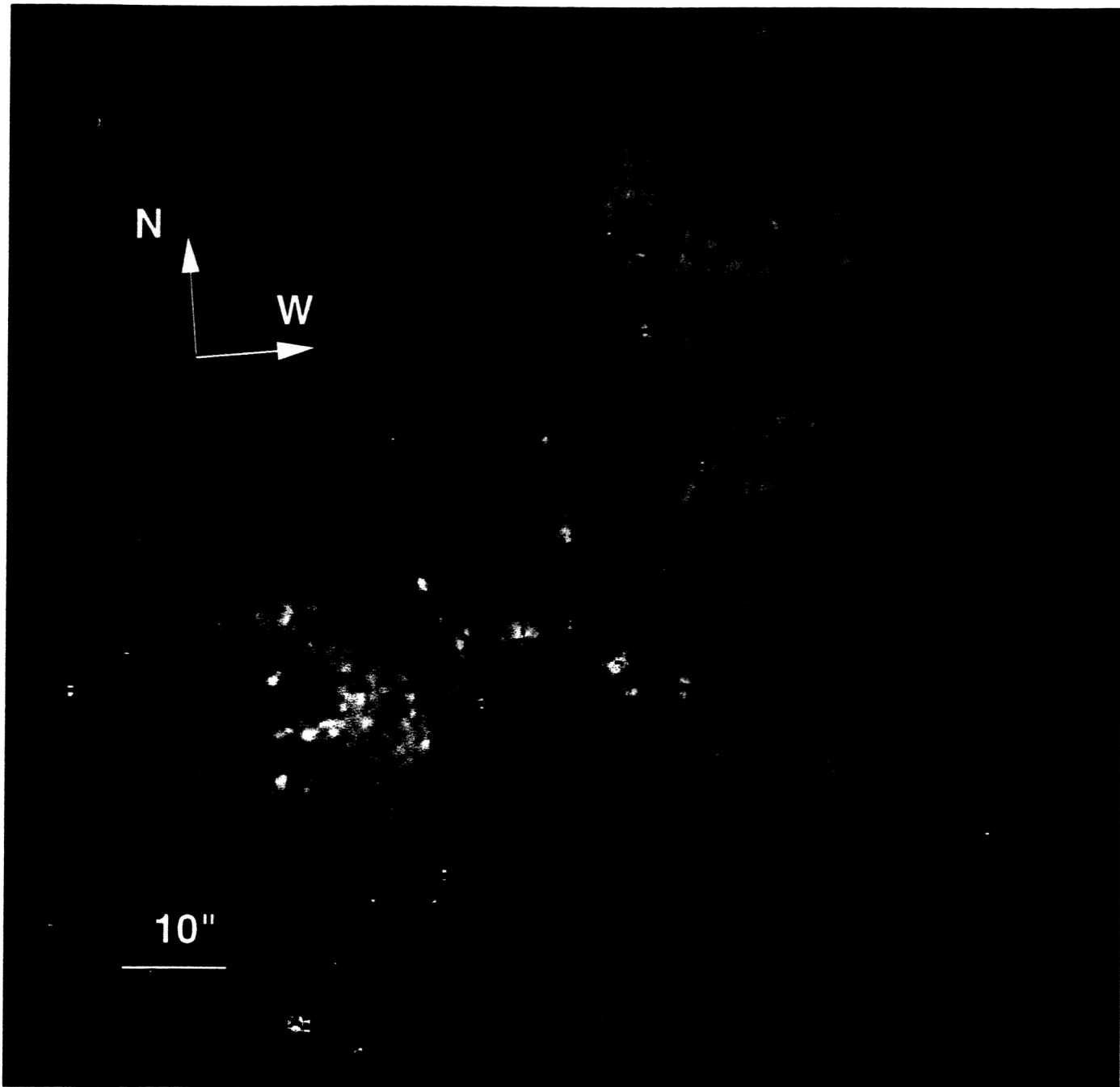


Fig 1



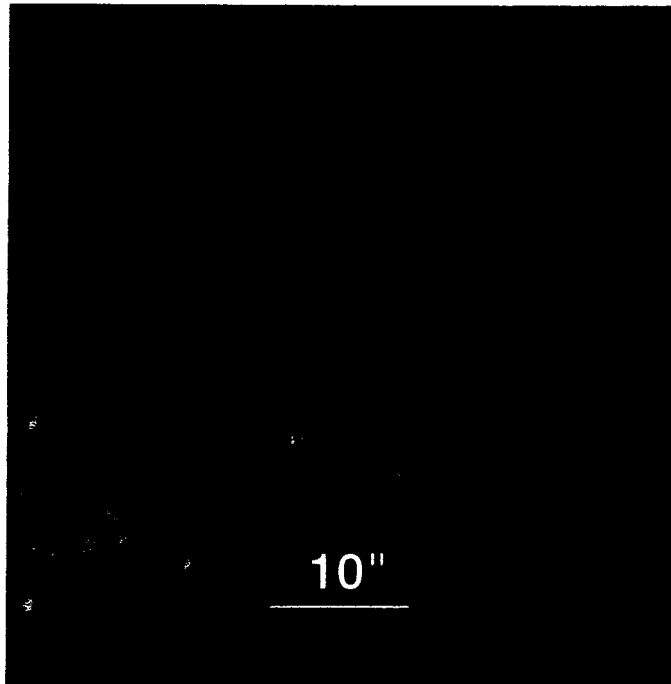
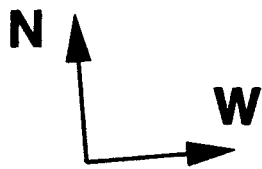
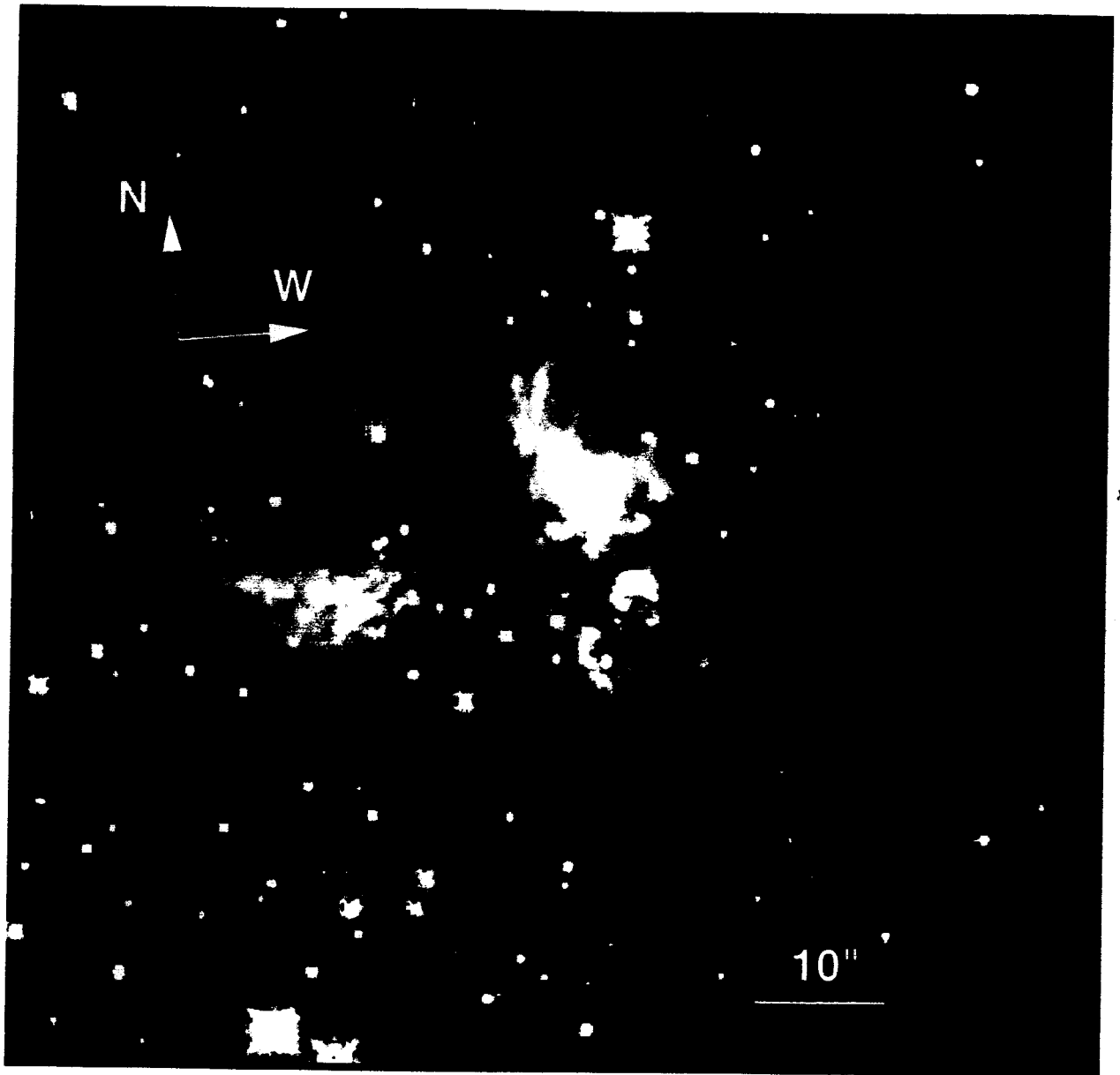


Fig 3



F

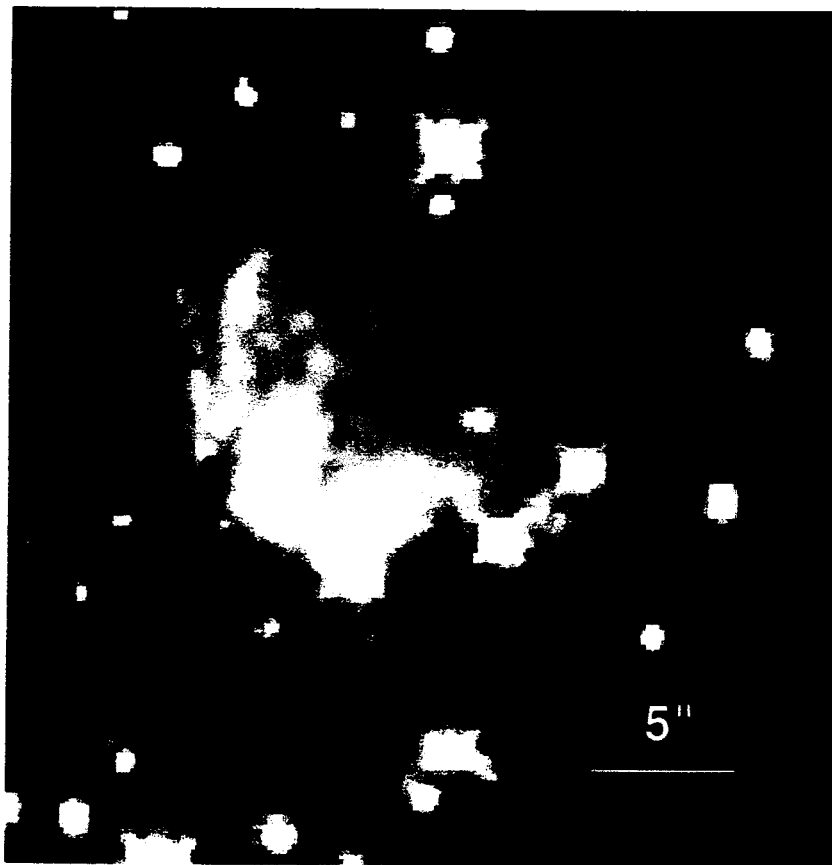
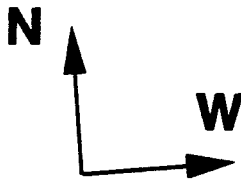


Fig 5